[CANCER RESEARCH 64, 2449–2460, April 1, 2004]

Transdominant ΔTAp73 Isoforms Are Frequently Up-regulated in Ovarian Cancer. Evidence for Their Role as Epigenetic p53 Inhibitors *in Vivo*

Nicole Concin,[1,2] Kirsten Becker,[1] Neda Slade,[1] Susan Erster,[1] Elizabeth Mueller-Holzner,[2] Hanno Ulmer,[3] Guenter Daxenbichler,[2] Alain Zeimet,[2] Robert Zeillinger,[4] Christian Marth,[2] and Ute M. Moll[1]

[1]Department of Pathology, State University of New York at Stony Brook, Stony Brook, New York; [2]Abteilung für Gynäkologie und Geburtshilfe and [3]Biostatistisches Institut, Universität Innsbruck, Innsbruck, Austria; [4]Obstetrics and Gynecology, University of Vienna and Ludwig-Boltzmann-Institute for Gynecology and Gynecological Oncology, Vienna, Austria

ABSTRACT

Despite strong homology, the roles of TP53 and TP73 in tumorigenesis seem to be fundamentally different. In contrast to TP53, tumor-associated overexpression of TP73 in many different cancers, combined with virtual absence of inactivating mutations and lack of a cancer phenotype in the TP73 null mouse are inconsistent with a suppressor function but instead support an oncogenic function. The discovery of NH_2-terminally truncated p73 isoforms, collectively called ΔTAp73, is now the focus of intense interest because they act as potent transdominant inihibitors of wild-type p53 and transactivation-competent TAp73. Therefore, establishing deregulated ΔTAp73 expression in tumors could be the crucial link to decipher which of the two opposing roles of this bipolar gene is the biologically relevant one. This study is the largest to date and encompasses 100 ovarian carcinomas with complete expression profile of all NH_2-terminal isoforms, discriminating between TAp73 and ΔTAp73 (ΔNp73, ΔN′p73, Ex2p73, and Ex2/3p73) by isoform-specific real-time reverse transcription-PCR. We find that the set of NH_2-terminal p73 isoforms distinguishes ovarian cancer patients from healthy controls and thus is a molecular marker for this diagnosis. Ovarian cancers strongly and almost universally overexpress ΔN′p73 compared with normal tissues (95% of cancers). About one-third of tumors also exhibit concomitant up-regulation of the antagonistic TAp73, whereas only a small subgroup of tumors overexpress ΔNp73. Thus, deregulation of the E2F1-responsive P1 promoter, rather than the alternate P2 promoter, is mainly responsible for the production of transdominant p53/TAp73 antagonists in ovarian cancer. Tumor stage, grade, presence of metastases, p53 status, and residual disease after resection are significant prognostic markers for overall and recurrence-free survival. A trend is found for better overall survival in patients with low expression of ΔN′p73/ΔNp73, compared with patients with high expression. A strong correlation between deregulated ΔTAp73 and p53 status exists. p53 wild-type cancers exhibit significantly higher deregulation of ΔN′p73, ΔNp73, and Ex2/3p73 than p53 mutant cancers. This data strongly supports the hypothesis that overexpression of transdominant p73 isoforms can function as epigenetic inhibitors of p53 *in vivo*, thereby alleviating selection pressure for p53 mutations in tumors.

INTRODUCTION

TP73 is a new family member of *TP53*, one of the most important tumor suppressor genes in human cancer. Significant structural homology exists between p73 and p53. The human full-length p73, mainly TAp73α and TAp73β (two COOH-terminal splice variants) largely mimic p53 function in experimental systems. p73 activates many of the p53 cellular target genes and is capable of inducing cell cycle arrest and apoptosis (1–3). Moreover, endogenous TAp73 is able to integrate several p53-dependent death stimuli. For example, DNA-damaging agents, such as cisplatin and γ-ionizing radiation (4–6) as well as oncogenes like E2F1, cMyc, and E1A (7–10) have been found to activate endogenous TAp73.

However, the roles of TP53 and TP73 in mammalian tumorigenesis seem to be fundamentally different. In sharp contrast to TP53, the virtual absence of inactivating mutations in over 1,100 human tumors screened to date (11), combined with tumor-associated overexpression of wild-type TP73 in many different types of human cancers as well as the lack of a cancer phenotype in the TP73 knockout mouse (12), are all inconsistent with a suppressor function. Moreover, the classic viral oncoproteins SV40 T antigen, Ad E1B 55 kDa, and human papillomavirus E6, which all target and inactivate p53 during host cell transformation, do not target the TAp73 protein physically or functionally (reviewed in Ref. 13). One possible explanation for the different roles of p53 and p73 in tumorigenesis lies within the different genomic organization of these genes. Whereas p53 encodes one protein, TP73 gives rise to several different NH_2 (and COOH-terminal) isoforms with opposing functions. The discovery of an NH_2-terminally truncated, transactivation-deficient dominant-negative p73 isoform in the mouse shifted the interest toward the p73 NH_2 terminus (14). This so-called ΔNp73 protein plays an essential antiapoptotic role during development of the central and autonomous nervous system by counteracting developmental p53-mediated neuronal death. Aside from the proapoptotic, transactivation-competent TAp73 with a putative suppressor role, four different NH_2-terminally truncated isoforms (ΔNp73, ΔN′p73, Ex2p73, and Ex2/3p73) have now been found in human cancers and/or cancer cell lines (see Fig. 1*A*). Each of these isoforms lack all or most of the transactivation domain and therefore are collectively called ΔTAp73. ΔTAp73 products are generated either via alternative exon splicing of the P1 promoter transcript (producing ΔN′p73, Ex2p73, and Ex2/3p73; Refs 15–18) or via alternative use of the P2 promoter in intron 3 (producing ΔNp73; Ref. 19). The Ex2p73 and Ex2/3p73 isoforms lack either exon 2 or exons 2/3, respectively. Of importance, the transcripts ΔNp73 and ΔN′p73 encode the same protein product. ΔTAp73 isoforms fail to induce cell cycle arrest and apoptosis (19–21). Their biological importance might lie in the fact that ΔTAp73 proteins retain their DNA-binding and tetramerization competence and thus can act as powerful dominant-negative inhibitors of both wild-type p53 and TAp73 in primary and transformed cells (15, 17–19, 22).

Evidence is mounting that ΔTAp73 might indeed act as a biologically relevant oncogene in primary human cancer. In cultured human cancer cells, ΔNp73 inhibits the suppressive activity of p53 and TAp73 in colony formation assays (19). ΔTAp73 overexpression results in malignant transformation of immortalized NIH3T3 fibroblasts *in vitro* that produce tumors in nude mice (18). ΔNp73 promotes immortalization in primary cells and cooperates with oncogenic Ras to drive their transformation *in vivo* (23). Also, ΔTAp73 could mediate hyperphosphorylation of Rb, resulting in enhanced E2F activity, opening the possibility that ΔTAp73 might also interfere with the Rb tumor suppressor pathway (24). Lastly, in the first clinical study on the impact of ΔNp73 expression in human cancer, ΔNp73 was an independent prognostic marker for reduced progression-free and overall survival in neuroblastoma patients (25).

Received 4/16/03; revised 1/2/04; accepted 1/27/04.

Grant support: Grants from the Fond zur Förderung Wissenschaftlicher Forschung to N. Concin, the National Cancer Institute and the United States Army Medical Research Command to U. Moll and the NY State Health Department.

The costs of publication of this article were defrayed in part by the payment of page charges. This article must therefore be hereby marked *advertisement* in accordance with 18 U.S.C. Section 1734 solely to indicate this fact.

Requests for reprints: U. M. Moll, Department of Pathology, BST 9, R134, State University of New York at Stony Brook, New York. Phone: (631) 444- 2459, Fax: (631)444-3424; E-mail: umoll@notes.ml.sunysb.edu.

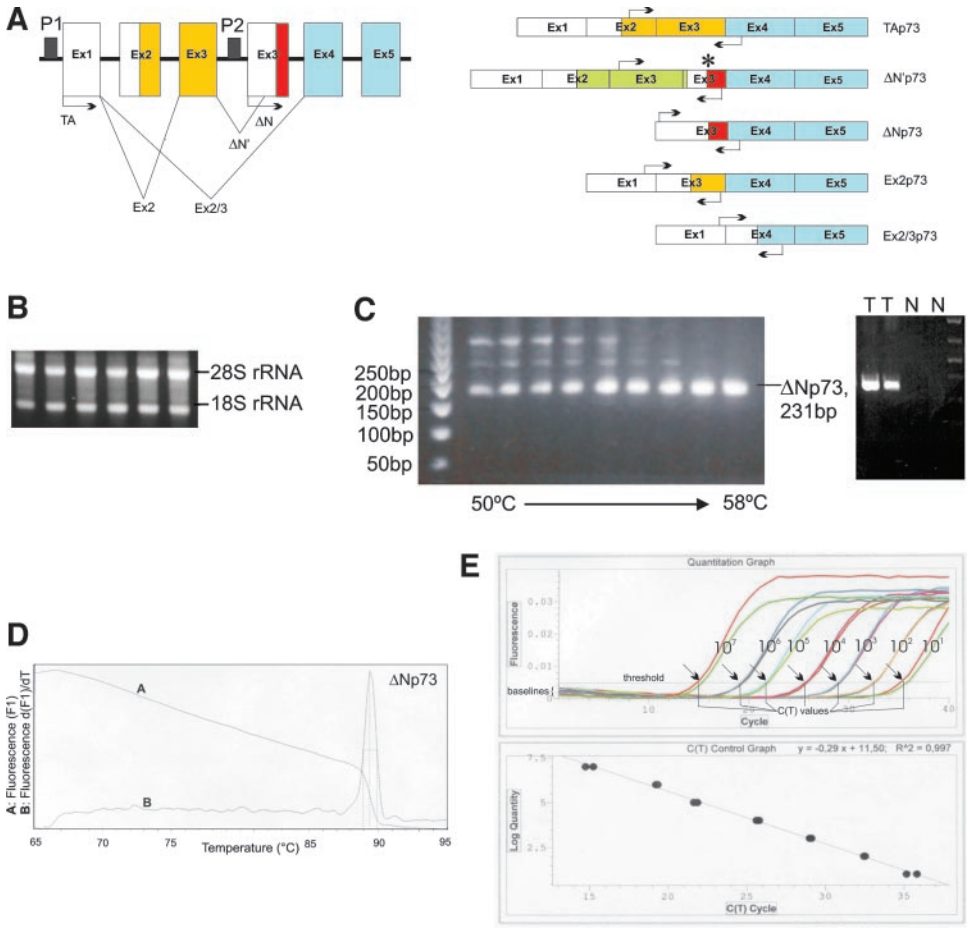

Fig. 1. *A*, the complete set of NH_2-terminal transcripts encoding TAp73 and ΔTAp73 isoforms. *Top*, gene architecture of the NH_2 terminus of *TP73*. The various isoforms are indicated. *Arrows* indicate transcriptional start sites. *Bottom*, positions of reverse transcription (RT)-PCR primers for the various p73 isoforms used in this study. The primer sequences are listed in Table 2. *White*, untranslated sequences; *yellow*, transactivation domain; *red*, exon 3′ derived coding sequences; *blue*, DNA-binding domain; *green*, translated (but nonproductive sequence) of ΔN′p73 that undergoes a premature stop in the 5′ untranslated region of exon 3′. The *star* indicates the used second translational start site in ΔN′p73. In ΔNp73, Ex2p73, and Ex2/3p73 translational start sites are indicated by *color borders*. *B*, examples of agarose gel electrophoresis of total RNA isolated from six ovarian carcinomas (1 μg of RNA/*Lane*). Distinct 28S and 18S bands indicate good quality. *C*, agarose gel electrophoresis of RT-PCR amplicons from a tumor RNA, generated with the ΔNp73 primers over a temperature gradient from 50 to 58°C. At low temperature, higher nonspecific bands are also present, which gradually vanish with increasing temperature until only the specific band (predicted size 231 bp) is generated. This amplicon was sequence confirmed to be ΔNp73. The same analysis was done for all isoforms. *Right*, cDNAs from two additional tumors and two normal tissues were subject to the RT-PCR reaction for ΔNp73 for 45 cycles at 58°C. *D*, *curve A*, melting curve of ΔNp73 amplicons generated at 58°C. The rapid fall-off at 89°C indicates the presence of a specific product that melts at this temperature. *Curve B*, the T_m of this specific product can be visualized more clearly when *curve A* is redrawn as a first-derivative plot, converting the drop into a peak. *E*, standard curve of copy numbers in real-time RT-PCR. Ex2p73 is shown as an example. *Top*, reactions with an Ex2p73 plasmid as template using 10-fold serial dilutions in duplicates. Ten copies of Ex2p73 transcripts were reproducibly detected. C(T) values indicate the cycle numbers at which the fluorescent signal crosses the threshold for a given copy number (*arrows*). *Bottom*, logarithmic plot of the Ex2p73 dilution curve. $R^2 = 0.997$.

Given these findings plus the overexpression of p73 in human tumors, the possibility arises that in fact the dominant-negative ΔTAp73 isoforms (rather than TAp73) might be the physiologically relevant components of p73 overexpression in tumors, functionally overriding an accompanying increase in TAp73 expression. The existence of this inhibitory family network could readily explain the paucity of p73 mutations in human tumors. Of note, many of the previous p73 overexpression studies in human cancers did not use primer pairs or antibodies specific for TA/ΔTAp73 isoforms and therefore determined the composite sum of p73 levels derived from all variants. Therefore, up-regulation of ΔTAp73 forms might have contributed to the elevated "p73" levels found previously in human cancers. Thus far, only a few studies, encompassing a very limited number of tumors, focused on the specific expression of ΔTAp73. In the largest such study that had taken place previously, we reported that ΔNp73 transcripts are overexpressed in 73% of 37 malignant gynecological tumors, compared with the patients' matched normal tissues of origin. Moreover, 31% of 52 breast cancers overexpressed ΔNp73 compared with normal breast tissue (19).

Therefore, a comprehensive and detailed survey of expression profiles is urgently needed to clarify if tumor-specific up-regulation of ΔTAp73 isoforms is a clinically important phenomenon in human cancers. This knowledge is critical for our understanding of the true role of TP73 in tumorigenesis. We therefore undertook this study, the largest and most detailed to date, in primary tumors and determined expression levels of all ΔTAp73 and TAp73 products. Using isoform-specific quantitative real-time reverse transcription (RT)-PCR, we analyzed 100 primary ovarian carcinomas and compared their various isoform mRNA levels to a group of 48 normal tissues. The results greatly substantiate the significance of deregulation of these dominant-negative inhibitors in human cancer and provide further support for an oncogenic role of TP73 in tumor formation.

MATERIALS AND METHODS

Tissue. Ovarian cancer tissues from 100 patients were collected during surgery at the Department of Obstetrics and Gynecology, University of Innsbruck, Austria, in compliance with and approved by the Institutional Review Board. Their histological subtypes are given in Table 1. Tissues were immediately snap frozen in liquid nitrogen, pulverized in the frozen status, and

Table 1 *Histological subtypes of 100 ovarian carcinomas used in this study*

Histological subtype	Number of tumors
Serous adenocarcinoma	35
Mucinous adenocarcinoma	39
Endometrioid adenocarcinoma	19
Clear cell adenocarcinoma	2
Undifferentiated carcinoma	1
Histological type not available	4

stored at −80°C until usage. Normal ovarian control tissues from 16 patients were obtained from the Southern Division of the Cooperative Human Tissue Network (Birmingham, Alabama). An additional 32 normal tissues were collected during surgery at Stony Brook University in compliance with and approved by the Institutional Review Board.

RNA Isolation and cDNA Preparation. RNA was extracted from tissue using the RNAeasy Mini Kit (Qiagen Sciences, Germantown, MD). High RNA quality was confirmed by Tris-acetate-EDTA agarose gel electrophoresis (Fig. 1*B*). Total RNA (5 μg) was reverse transcribed using the Thermo Script RT-PCR system (Invitrogen) and random primers.

Primer Design. Primer pairs for TAp73, Ex2p73, and Ex2/3p73 were designed using Gene Runner version 3.05 and Primer Picking Software (http://www.genome.wi.mit.edu7cgi-bin/primer/primer3_www.cgi). Several different primer pairs for each of these isoforms were designed and tested before the optimal ones were chosen for all additional experiments. Primers for ΔNp73 and ΔN′p73 were used as described previously (18).

All primer pairs detected a unique specific cDNA (see Fig. 1*A*). For TAp73, Ex2p73, and Ex2/3p73, primers spanning splice junctions were used. For ΔNp73, the upstream primer detected a sequence unique for this transcript (5′ untranslated region of exon 3′). Specificity for ΔN′p73 was achieved by the unique combination of the upstream and downstream primer. Specificity of each primer pair was confirmed by detecting single bands of amplicons on agarose gels (Fig. 1*C*) and by sequencing the PCR products. Also, all primers were queried against the nonredundant Human Genome Database (National Center for Biotechnology Information). In no case were unrelated gene matches found. Although two nonpaired primers matched to the related TP63 gene, their respective return primer did not. Table 2 lists all primer pairs for the five examined p73 isoforms and for the internal normalizer 28S rRNA.

Real-Time RT-PCR. Absolute copy numbers for all isoforms were determined by real-time RT-PCR using the SYBR Green Dye method (Qiagen Sciences). 28S rRNA was used to normalize samples (26). PCR reaction was performed in a 20-μl reaction mixture containing 1/32 of the reverse transcription reaction, 10 μl of QuantiTect SYBR Green PCR Master Mix, and 6.25 pmol of each primer. The Master Mix is a premixed solution containing HotStartTaq DNA Polymerase, QuantiTect SYBR Green PCR buffer, deoxynucleoside triphosphates, SYBR Green I, and ROX (a passive reference dye). The PCR conditions were as follows: initial melting at 95°C for 15 min followed by 39 cycles of 94°C denaturation for 30 s; annealing for 30 s; elongation at 72°C for 1 min; and plate reading for 10 s (plate reading temperature was set 2.5°C below the pre-established melting temperature of each PCR product). Annealing temperatures were optimized by running temperature gradient PCR reactions (Fig. 1*C*). Annealing and melting temperatures for each PCR product are shown in Table 3. Melting curves for each PCR product were then generated; an example is shown in Fig. 1*D*. Data were collected using the DNA Engine Opticon (MJ Research, Waltham, MA), a 96-wellplate-based continuous fluorescence detection system. Each sample was tested in duplicate, and a negative control was included on every plate. An increase in fluorescence above baseline indicated the accumulation of a specific PCR product. Its threshold was set above the baseline and in the exponential phase of the PCR. The computed tomography value was defined as the cycle number at which the fluorescence crossed the threshold.

Standard Curves. To determine the absolute copy numbers of p73 isoforms, PCR products for each isoform were cloned into the pCR II vector using the TA Dual Promoter Cloning Kit (Invitrogen). Constructs were verified by sequencing. A pBR322-based vector containing the 28S rRNA cDNA insert was a gift from G. Zambetti (St. Jude Children's Research Hospital). Cloned plasmids were linearized, and their concentrations were carefully measured by UV spectrophotometry to allow copy number determination. Ten-fold serial dilutions were made ranging from 10 to 10 million copies for each p73 isoform plasmid and from 1000 to 1000 million copies for the 28S rRNA containing plasmid. Our assay allowed the reproducible detection of as low as 10 copies of p73 mRNA transcripts for each isoform; thus the dynamic range of the standard curves spanned at least seven orders of magnitude (Fig. 1*E*). After normalization of each sample to its own 28S rRNA transcript level, data were expressed as absolute copy numbers per 154 ng of total RNA.

Western Analysis. Frozen pulverized tumor tissue was suspended in 1.5 ml of TENN buffer [50 mM Tris, 5 mM EDTA, 150 mM NCL, 0.5% NP40 (pH8.0)] containing a protease inhibitor mixture (Roche) and homogenized by sonication. Lysates were centrifuged twice at 14,000 rpm for 15 min, and supernatants were loaded onto 10% SDS-PAGE gels. Membranes were immunoblotted with the p73β antibody GC15 (Calbiochem) at 1:40. For comparison, a normal tissue pool was generated by mixing equal ratios of 12 normal ovarian tissues. Normal ovarian tissue samples were also analyzed separately and found to show little differences in expression level from sample to sample.

Yeast-Based Assay for p53. To detect inactivating mutations in the *p53* gene, the functional yeast-based assay was used as described previously (27). Briefly, the functional analysis of separated alleles in yeast is based on transcriptional activity of wild-type *versus* mutant p53 alleles in a yeast reporter system. p53 mRNA species from tumors were reverse transcribed, amplified by PCR, and cotransformed into *Saccharomyces cerevisiae* together with a linearized yeast homologous recombination expression vector carrying the 5′ and 3′ ends of the *p53* open-reading frame. Wild-type p53, which activates transcription of the yeast ADE2 gene that encodes the phosphoribosylaminoimidazole carboxylase results in white colonies, whereas mutant alleles lack transcriptional activity and result in smaller, red colonies.

Statistical Analyses. The data distribution of normalized expression levels for both the ovarian cancer group and the normal tissue group was non-Gaussian. Therefore, nonparametric tests were applied for data analysis. The fold up-regulation of each p73 isoform in tumors was calculated in reference to the median expression level of the entire normal tissue group. Up-regulation in a given tumor was defined as expression levels above the 75th percentile of median expression level of the normal tissue group. Correspondingly, down-regulation in a given tumor was defined as expression levels below the 25th percentile of the median expression level of the normal tissue group. In all classes of p73 isoforms, a few cases fell into the upper or lower "outlier" group in both the normal and the tumor group. The latter was defined as 1.5-fold above or below the 75th and 25th percentile values, respectively, and are indicated (Fig. 3*A*, *black circles*). The Mann-Whitney *U* test was used for comparing p73 isoform expression of tumor and normal tissues and for correlation analysis of p73 isoform expression with p53 mutational status (Figs. 3*A* and 5). For correlations among the various p73 isoforms, data were logarithmized that produced a Gaussian distribution, and the Spearman correlation test was applied. P values < 0.05 were considered statistically significant.

Clinical Data. Clinical data of 96 ovarian carcinoma patients were available. All patients were treated at the Department of Obstetrics and Gynecology, University of Innsbruck, Austria, between May 1991 and June 2001.

Table 2 *Primer pairs for p73 isoforms and for the internal standard 28 SrRNA*

	Sense	Antisense	Amplicon size
Ex2p73	GACGGCTGCAGGGAACCAGA	TGCCCTCCAGGTGGAAGACG	115 bp
Ex2/3 p73	TGCAGGCCCAGTTCAATCTGC	TCGGTGTTGGAGGGGATGACA	178 bp
ΔNp73	CAAACGGCCCGCATGTTCCC	TTGAACTGGGCCGTGGCGAG	231 bp
ΔN′p73	TCGACCTTCCCCAGTCAAGC	TGGGACGAGGCATGGATCTG	211 bp
TAp73	GCACCACGTTTGAGCACCTCT	GCAGATTGAACTGGGCCATGA	167 bp
28S rRNA	TTGAAAATCCGGGGGAGAG	ACATTGTTCCAACATGCCAG	100 bp

Table 3 *Annealing and melting temperatures for p73 isoforms and 28S rRNA internal control*

	Annealing temperature	Melting temperature
Ex2p73	56.8°C	83.0°C
Ex2/3 p73	55.3°C	88.5°C
ΔNp73	58.0°C	89.0°C
ΔN′p73	59.0°C	87.5°C
TAp73	51.5°C	83.5°C
28S rRNA	57.0°C	81.8°C

Ninety-four of the 96 patients underwent tumor resection, whereas two patients were treated with carboplatin monotherapy only because of advanced age and impaired general health. Surgical treatment included total hysterectomy and bilateral salpingo-oophorectomy in all but two patients. Eighty of the 94 patients underwent additional omentectomy, and partial bowel resection was necessary in 13 patients. Lymph node evaluation involved pelvic lymphadenectomy in 37 of 94 patients.

The median age at the time of diagnosis was 62 (range, 24 to 90) years. Patients presented with International Federation of Gynecologists and Obstetricians' stage I ($n = 20$), stage II ($n = 5$), stage III ($n = 58$), and stage IV ($n = 11$) at the time of diagnosis. In two cases, the International Federation of Gynecologists and Obstetricians' stage was unknown. To classify tumor grade, the widely used system based on architectural and nuclear grade and mitotic activity was applied. Distant metastases were seen in 11 patients at the time of diagnosis [lung ($n = 1$), pleura ($n = 5$), liver ($n = 3$), skin ($n = 1$), and others ($n = 3$)]. With the exception of seven patients with stage I carcinomas, all patients received adjuvant platinum-based chemotherapy. This involved four to six courses of carboplatin monotherapy ($n = 24$) or a combination therapy of cisplatin and cyclophosphamide ($n = 35$); cisplatin, carboplatin, and cyclophosphamide ($n = 9$); carboplatin and paclitaxel ($n = 20$); and cisplatin, paclitaxel, and cyclophosphamide ($n = 1$). During follow-up, 42 of 96 patients suffered recurrent ovarian cancer, and 54 of the 96 patients died. The median time of follow-up was 43 months (ranging from 3 to 154 months); the mean time of follow-up was 80 ± 30 months.

Survival probabilities were calculated by the product limit method of Kaplan and Meier. Differences between groups were tested using the log-rank test. The results were analyzed for the end point of overall and recurrence-free survival. Overall survival was defined as the time between diagnosis and death, regardless of the cause. Patients who had not died were censored at the last date they are known to have been alive. Recurrence-free survival was calculated from the day of diagnosis until the date when progressive disease, relapse, or death was reported, whichever occurred first. Patients who had not experienced any unfavorable event were censored at the last date they were known to have been alive. The Cox proportional hazards model was used for multivariate analysis to assess the independence of different prognostic factors.

RESULTS

The Set of NH_2-Terminal p73 Isoforms Distinguishes Ovarian Cancer Patients from Healthy Controls. After validation of the isoform-specific real-time RT-PCR (examples are shown in Fig. 1), we determined the p73 expression profiles of TAp73 and all four ΔTA isoforms in 100 primary ovarian carcinomas and compared them to 48 normal ovarian and other tissues (Fig. 3*A*, *linear scales*, *left*, and *logarithmic scales*, *right*). Of note, we showed previously in 50 different adult and fetal tissues including ovaries that total p73 levels varied only minimally (<4-fold; Ref. 28). All data were normalized to the tissues' own internal control of 28S rRNA cDNA. Moreover, the 28S rRNA cDNA levels in tumors were very similar compared with the normal tissue group (Fig. 3*A*, *top box plot*). Therefore, the raw data changed only slightly after normalization for 28S rRNA. Absolute copy numbers, expressed per standard input total RNA (154 ng), were then calculated for all isoforms.

Using this comprehensive data set, we first analyzed whether the entire five-variable set of p73 isoforms correlates with the presence or absence of disease. A few individuals were excluded because of incomplete data sets for all five variables, leaving 94 patients and 45 normal controls. To this end, a correlation matrix was calculated as follows: first, patients and controls were combined into one group; next, each individual (i) in the combined group was assigned a five component vector V(i), composed of v_{1i} = TAp73, v_{2i} = ΔN′p73, v_{3i} = ΔNp73, v_{4i} = Ex2p73, and v_{5i} = Ex2/3p73. To look for similarities or dissimilarities within that combined group, a correlation matrix was calculated. This quantifies the similarity of parameters v_{1-5}, between every possible pair of individuals (i) and (j). Fig. 2*A* shows the contour plot of the resulting correlations that are higher than 0.990. Axes *X* and *Y* plot individuals for pairwise comparison

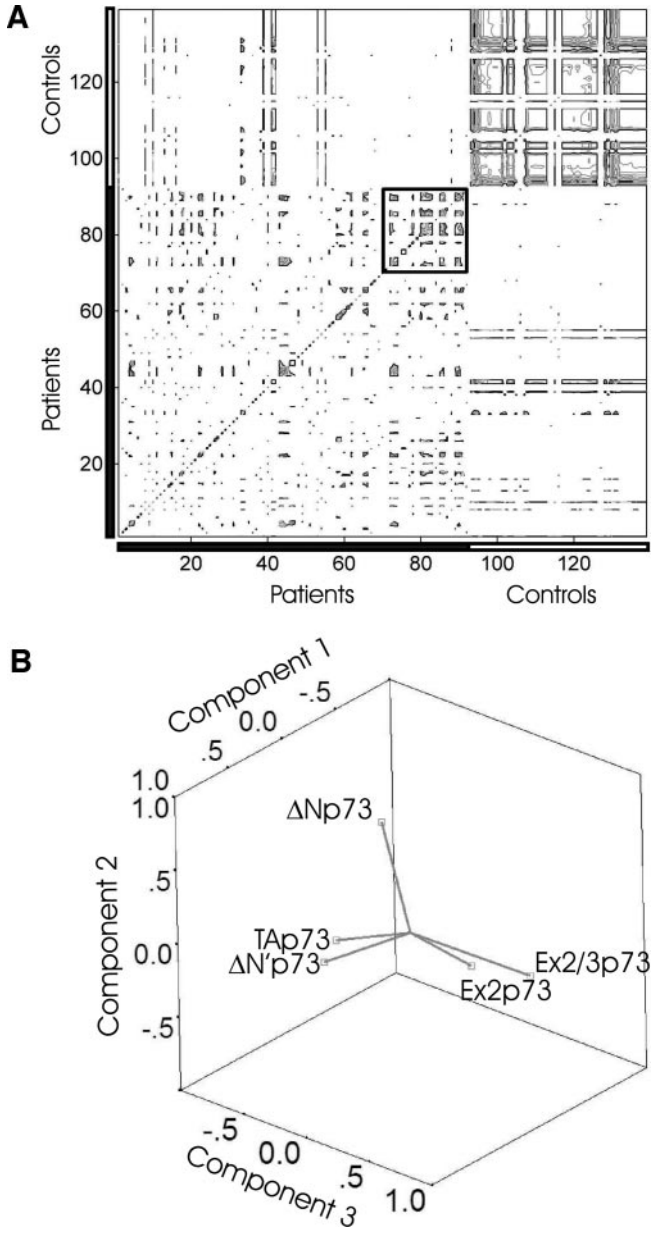

Fig. 2. *A*, the set of NH_2-terminal p73 isoforms distinguishes ovarian cancer patients from healthy controls. Correlation matrix between p73 levels and disease state. Patients and controls were each assigned a five component vector V(i), composed of v_{1i} = TAp73, v_{2i} = ΔN′p73, v_{3i} = ΔNp73, v_{4i} = Ex2p73, and v_{5i} = Ex2/3p73. Axes *X* and *Y* plot individuals for pairwise comparisons i and j (*positions 1–94* are patients, *ordered by increasing survival time from left to right and bottom to top; positions 95–139* are normal controls). The contour plot of all correlations higher than 0.990 is shown. *B*, graphic representation of Principal Component Analysis with Varimax rotation. This analysis reveals that there are only three independent and statistically significant bits of information within the five components of the assay results. TAp73 and ΔN′p73 represent one independent component, ΔNp73 represents a second component, and Ex2/3p73 and Ex2p73 represent the third component.

(positions 1–94 are patients, ordered by increasing survival time from *left to right* or *bottom to top*; positions 95–139 are normal controls). As is clearly apparent in Fig. 2*A*, the set of p73 isoform values within the control group are strongly intercorrelated (*top right block*, characterized by *solid contours*). This quantifies the low person-to-person variation in levels of TAp73, ΔN′p73, ΔNp73, Ex2p73, and Ex2/3p73 isoforms within the control group. In contrast, the patient group is characterized by a high person-to-person variability in levels of TAp73, ΔN′p73, ΔNp73, Ex2p73, and Ex2/3p73 (*lower left block*). The high individuality of isoform levels within the patient group is revealed by the *scattered "dot"* character of the in-group correlations. Moreover, the patient group is uncorrelated with the control group, as revealed by virtually *empty off-diagonal areas* in positions 94–139. Interestingly though, the patient matrix does reveal a higher similarity in the p73 isoform contours within those patients who survive longest, compared with the remaining patients with shorter survival (subgroup of patients 70–94; see *small top right subset within the patient block*). Only nine patients exhibit some similarity to the control group (Fig. 2*A*, see the *off-diagonal contours* in the 95–139 area), indicating that in ~10% of cases, assaying for the set of p73 isoform levels alone might not reveal the presence of disease without additional indicators. Taken together, values of the five-variable set of p73 isoforms alone, without any additional clinical or pathological information about a person, clearly are able to discriminate the presence of ovarian cancer from its absence in about 90% of individuals.

To further analyze if there are interdependencies among the five-variable set of p73 isoforms within patients, the Principal Component Analysis with Varimax rotation was used, which is an established method of variance analysis. This analysis reveals that there are only three independent and statistically significant bits of information within the five components of the assay results (v_{1i} = TAp73, v_{2i} = ΔN′p73, v_{3i} = ΔNp73, v_{4i} = Ex2p73, and v_{5i} = Ex2/3p73; Fig. 2*B*). TAp73 and ΔN′p73 represent one independent component, ΔNp73 represents a second component, and Ex2/3p73 and Ex2p73 represent the third component. This statistical grouping correlates well with the predicted molecular grouping that derives from the two promoters and the gene architecture.

Ovarian Cancers Select for Deregulated Expression of Dominant-Negative ΔTAp73. Next, individual isoforms were analyzed. Consistent with previous reports in other tumor types, significant tumor-specific up-regulation was found for TAp73 (Fig. 3*A*, *second row box plots*). In contrast, expression levels of p73 in normal tissues were very low albeit somewhat scattered, with a median of 34 copies of TAp73 ($P < 0.05$). The median up-regulation in tumors was 11-fold (median of 357 copies of TAp73) compared with normal tissues, with a range up to 233-fold above the median normal. Thus, TAp73 up-regulation, defined as tumor levels ranging above the 75th percentile of normal tissue levels, was seen in 35% of ovarian cancers.

We next measured ΔN′p73. This isoform contains an additional 198 bp of the 3′ portion of exon 3′ via an aberrant splice from exon 3 into exon 3′ (Fig. 1*A*). This leads to an upstream premature stop, but a second translational start site within exon 3′ is productive. The ΔNp73 transcript contains an additional 78 bp region at the 5′ end of exon 3′ that is missing from ΔN′p73. However, at the translational level, both ΔNp73 and ΔN′p73 transcripts encode the same protein product, for which an oncogenic potential has been described (15, 18). Significantly, in our series of 100 ovarian cancers we found an almost universal prevalence of tumor-specific up-regulation of ΔN′p73, compared with normal tissue ($P < 0.05$; Fig. 3*A*, *third row box plots*). In the normal tissue group, the median copy number of ΔN′p73 transcripts was zero, and the range was rather narrow. In fact, in 59% (28 of 44) of normal tissues, no ΔN′p73 transcripts could be detected. In tumors, the median ΔN′p73 copy number was 65, ranging up to 1,325 copies. Thus, up-regulation of ΔN′p73, defined as tumor levels ranging above the 75th percentile of normal levels, was present in 95% (94 or 99) of ovarian cancers.

In contrast, tumors showed no median up-regulation of ΔNp73, although some individual tumors did exhibit increased levels (Fig. 3*A*, *fourth row box plots*). The median tumor level was similar to the median normal level (15 copies in tumors *versus* 12 copies in normal tissues). Only 26% (26 of 100) of tumors exhibited up-regulation of ΔNp73 (above the 75th percentile of the normal group). Within this up-regulated subgroup of tumors, the median up-regulation was 17-fold, with levels ranging up to 246-fold above the median normal. In contrast, the median up-regulation in normal tissues above the 75th percentile was only 11-fold. Within tumors, 6% (6 of 100) showed ΔNp73 expression levels that exceeded the highest ΔNp73 values found in the normal group.

Tumors did not up-regulate Ex2p73 (Fig. 3*A*, *bottom row box plots*). Although the median level in the tumor group was slightly lower (2-fold) than in the normal group, this difference was not significant (21 copies in tumors *versus* 46 copies in normal, $P = 0.132$). None of the ovarian carcinomas expressed Ex2p73 levels that exceeded the highest normal value.

For Ex2/3p73 transcripts, tumors exhibited strong and significant down-regulation compared with normal tissues (median of 393 copies in tumors *versus* 3162 copies in normal; $P < 0.05$; Fig. 3*A*, *fifth row box plots*). Interestingly, Ex2/3p73 showed a very wide range of expression within the normal group, varying 7,027-fold from the lowest to highest level measured. Median expression levels in the normal group were 8-fold higher than in the tumor group. Down-regulation (below the 25th percentile of the normal group) was seen in 57% (57 of 100) of tumors with a maximum down-regulation of 132-fold below the mean normal.

Thus, taken together, the strongest and most prevalent tumor-specific increase in expression was seen for ΔN′p73, with the great majority of tumors showing up-regulation. In ovarian cancer, this parameter stands out among all other p73 isoforms and serves as a molecular marker of this disease. About one-third of the tumors also exhibit concomitant up-regulation of the antagonistic TAp73. Only a small subgroup of tumors showed ΔNp73 up-regulation. In contrast, Ex2p73 and Ex2/3p73 levels either tended to be slightly lower in tumors (Ex2) or showed significant tumor-specific down-regulation (Ex2/3).

To verify that tumor transcript levels translated into respective protein levels in tumors, select tumors were analyzed by Western blot with the TAp73β-specific antibody GC15. Among all available p73 antibodies, GC15 is the most sensitive. As shown in Fig. 3*B*, protein levels correlated semiquantitatively with RT-PCR data for TAp73. On a transcript level, tumor 1 showed no overexpression, whereas tumors 2 and 3 showed strong and moderate overexpression of TAp73 transcripts, respectively. However, the complete set of NH_2-terminal p73 isoforms cannot be measured on a protein level because no specific antibodies of sufficient quality for any of the ΔTAp73 forms currently exist.

Frequent Concomitant Up-regulation of NH_2-Terminal p73 Isoforms in Individual Ovarian Cancers. When individual tumors were analyzed for coexpression of various NH_2-terminal p73 isoforms, significant co-up-regulation of isoforms was found in tumors ($P < 0.05$; Fig. 4). In contrast, only select correlations were present within the normal tissue. In tumors, the strongest correlation existed between TAp73 and ΔN′p73 (Fig. 4, *top left panel*). Here, the higher the TAp73 expression level in a given tumor, the higher the ΔN′p73 expression level within the same tumor (Pearson correlation coefficient $r = 0.829$; $P < 0.001$). This was also the case for the relationship between TAp73 and ΔNp73, albeit this correlation was not as strong (Fig. 4, *second left panel*; Pearson correlation coefficient

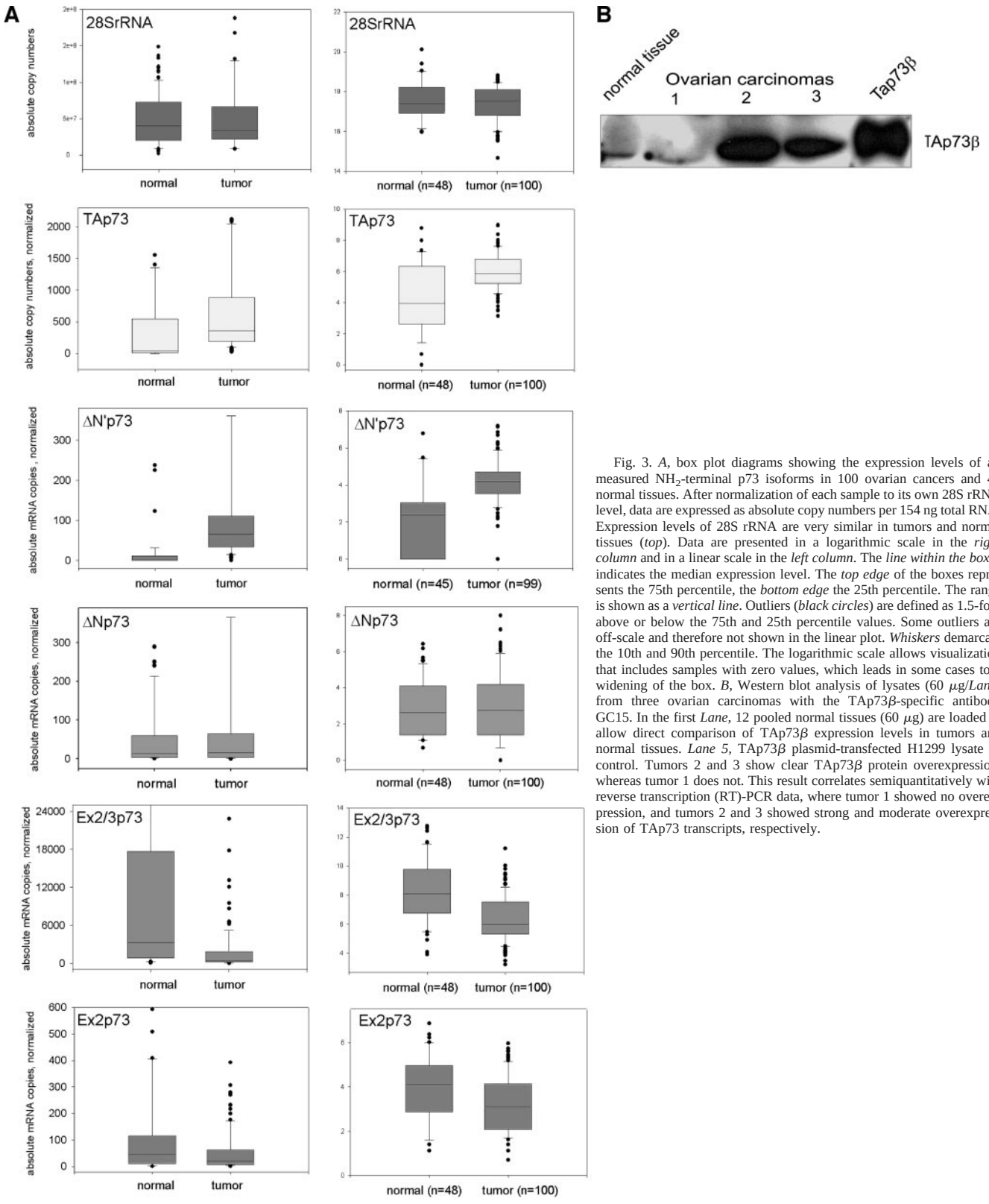

Fig. 3. *A*, box plot diagrams showing the expression levels of all measured NH_2-terminal p73 isoforms in 100 ovarian cancers and 48 normal tissues. After normalization of each sample to its own 28S rRNA level, data are expressed as absolute copy numbers per 154 ng total RNA. Expression levels of 28S rRNA are very similar in tumors and normal tissues (*top*). Data are presented in a logarithmic scale in the *right column* and in a linear scale in the *left column*. The *line within the boxes* indicates the median expression level. The *top edge* of the boxes represents the 75th percentile, the *bottom edge* the 25th percentile. The range is shown as a *vertical line*. Outliers (*black circles*) are defined as 1.5-fold above or below the 75th and 25th percentile values. Some outliers are off-scale and therefore not shown in the linear plot. *Whiskers* demarcate the 10th and 90th percentile. The logarithmic scale allows visualization that includes samples with zero values, which leads in some cases to a widening of the box. *B*, Western blot analysis of lysates (60 μg/*Lane*) from three ovarian carcinomas with the TAp73β-specific antibody GC15. In the first *Lane*, 12 pooled normal tissues (60 μg) are loaded to allow direct comparison of TAp73β expression levels in tumors and normal tissues. *Lane 5*, TAp73β plasmid-transfected H1299 lysate as control. Tumors 2 and 3 show clear TAp73β protein overexpression, whereas tumor 1 does not. This result correlates semiquantitatively with reverse transcription (RT)-PCR data, where tumor 1 showed no overexpression, and tumors 2 and 3 showed strong and moderate overexpression of TAp73 transcripts, respectively.

$r = 0.634$; $P < 0.001$). Nevertheless, 17 of 21 tumors with the highest ΔNp73 levels also exhibited high TAp73 levels; in addition, 8 of these 17 tumors were wild type for p53 (see below). The weakest correlations existed between TAp73 and Ex2p73 or Ex2/3p73 (*third left panel* and data not shown).

In contrast to tumors, normal tissues showed no correlation between TAp73 and ΔN′p73 expression levels, supporting the significance of tumor-specific co-up-regulation (Fig. 4, *top right panel*). Also, no correlation existed between ΔN′p73 and Ex2p73 or Ex2/3p73 levels. However, in normal tissues, Ex2p73 and Ex2/3p73 levels correlated with each other, and ΔNp73 levels correlated with ΔN′p73, Ex2p73, and Ex2/3p73 levels (data not shown).

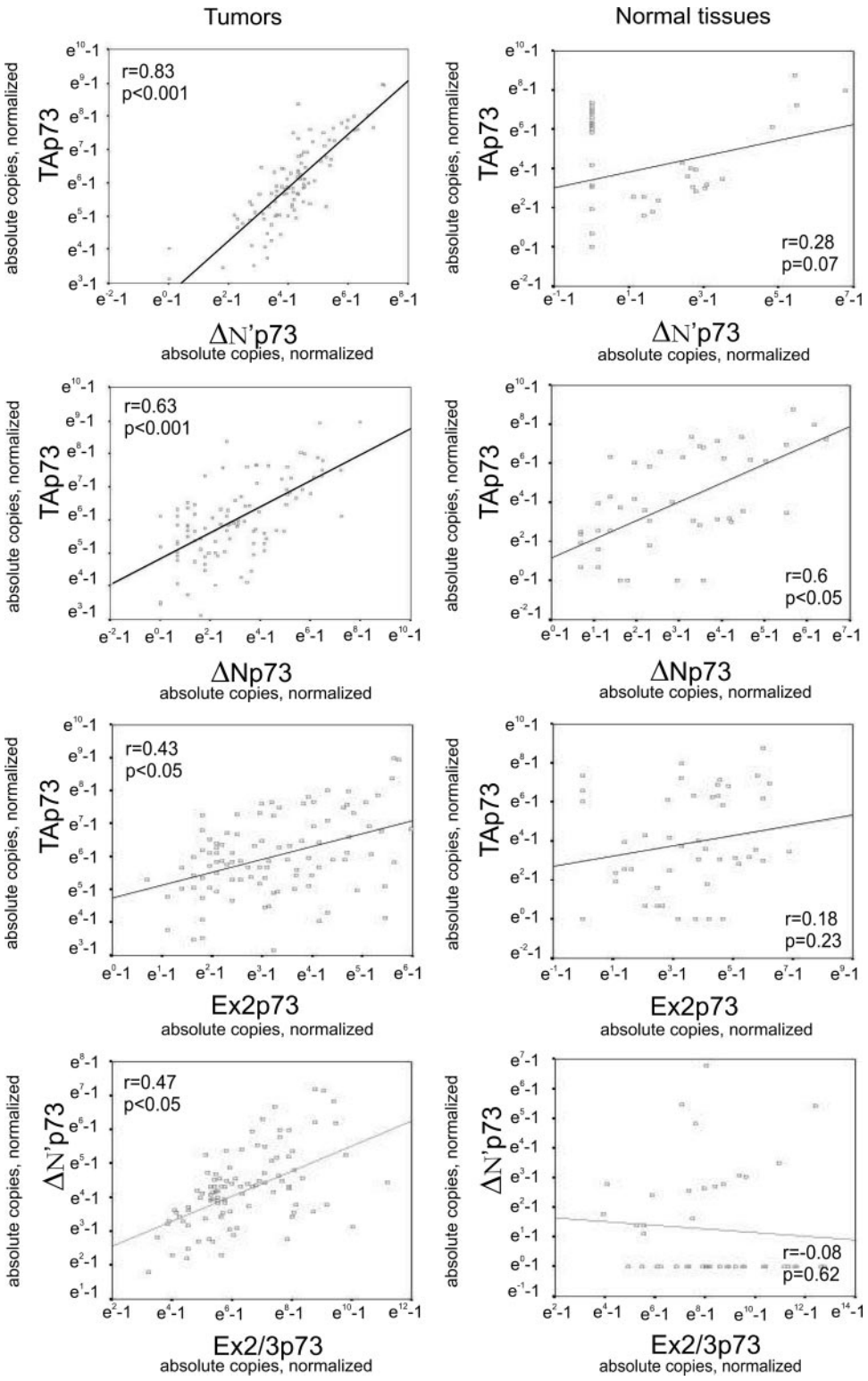

Fig. 4. Scatter plots of 100 ovarian cancers (*left column*) and 48 normal tissues (*right column*) analyzing correlations between TAp73 and various ΔTAp73 isoforms. Each *dot* represents a specific sample. Data are given in a logarithmic scale. A Pearson correlation coefficient (*r*) with values close to +1 indicates a perfect linear correlation, indicating co-up-regulation.

In summary, correlation analysis for coexpression of p73 isoforms within the tumor and normal groups highlights the difference in their expression patterns. As shown in Fig. 4, the correlation between TAp73 and ΔN′p73 is positive for tumors but negative for normals; the correlation between TAp73 and ΔNp73 is positive for tumors and for normals; the correlation between TAp73 and Ex2p73 is positive for tumors but negative for normals; and the correlation between ΔN′p73 and Ex2/3p73 is positive for tumors but negative for normals.

Wild-Type p53 Status Correlates with Up-regulation of ΔTAp73 in Ovarian Cancer. We determined the p53 mutation status in our tumor collection via a functional yeast-based assay. Of the 100 cases, we could ascertain the genotype in 93% (93 of 100). Of these, 74% (69 of 93) of tumors were identified as mutant p53, and 26% (24 of 93) were found to be wild type for p53. Of note, significantly higher expression levels of p53-inhibitory ΔTAp73 isoforms were found in p53 wild-type tumors, compared with p53 mutant

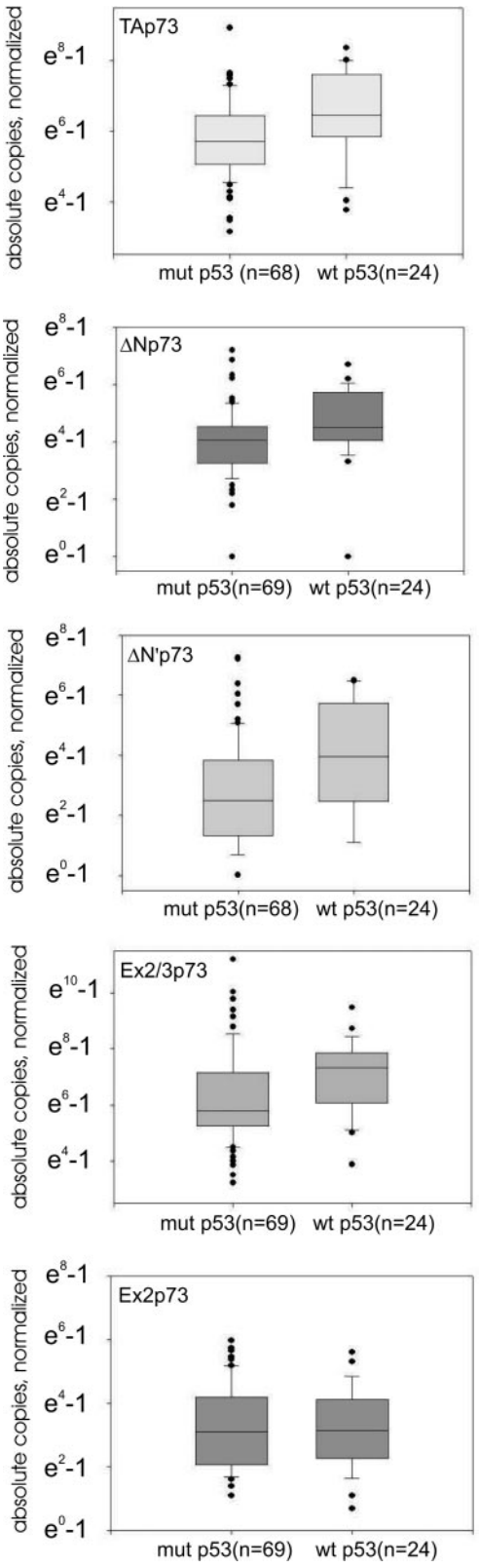

Fig. 5. Box plot diagrams as in Fig. 2*A*, showing the expression of all NH_2-terminal p73 isoforms in p53-mutated ovarian cancers compared with p53 wild-type ovarian cancers. Values were normalized for 28S rRNA.

tumors (Fig. 5). This was the case for ΔNp73, ΔN′p73, and to a lesser extent Ex2/3 p73 ($P < 0.05$ for all isoforms). Moreover, the prevalence of ΔNp73 and ΔN′p73 up-regulation (above the 75th percentile of the normal group) was higher in p53 wild-type tumors than in mutant tumors (Table 4). Although 23 and 82% of p53 mutant tumors exhibited up-regulation of ΔNp73 and ΔN′p73, 48% and 96% of p53 wild-type tumors exhibited up-regulation of ΔNp73 and ΔN′p73, respectively. On the other hand, no difference in the prevalence of TAp73 up-regulation existed between wild-type and mutant tumors (Table 4). However, in keeping with the isoform interrelatedness shown in Fig. 4, wild-type tumors expressed higher levels of TAp73 than mutant tumors (Fig. 5). No significant difference in Ex2/3 p73 expression was found between p53 wild-type and mutant tumors.

Clinicopathological Correlations. No significant correlation exists between p73 isoform levels in tumors and stage, grade, histological subtype, residual disease after resection, age, and distant metastases (Table 5). In contrast, p53 mutation status correlates significantly with tumor grade, histological subtype, and the presence of distant metastases at the time of diagnosis (Table 6). Although 91% of p53 wild-type tumors show moderate differentiation (grade 2), the majority of p53 mutant tumors (55%) show poor differentiation (grade 3). Also, the majority of p53 wild-type tumors were of mucinous types (64%). In contrast, the most common histological type of p53 mutant tumors was serous (42%), whereas only 34% of them were mucinous. Moreover, endometrioid tumors are 2.6 times more common in mutant than in wild-type tumors. None of the patients with p53 wild-type tumors presented with distant metastases at the time of diagnosis, whereas all 11 metastases occurred in patients with p53 mutant tumors. A strong trend was also seen for p53 mutation status with respect to residual disease after resection. In 87% (19) of patients with p53 wild-type tumors, complete macroscopic removal of tumor mass or at least debulking to <2 cm residual tumor could be achieved. Residual disease >2 cm was only seen in 14% (3) of p53 wild-type patients, in contrast to 39% (24) of patients with mutant tumors.

Survival Analysis. To determine the clinical impact of clinical parameters, p53 mutation status and p73 isoform expression levels in ovarian carcinoma, survival analyses were performed for recurrence-free and overall survival. As expected, in univariate analysis, tumor stage, grade, residual disease after resection, and the presence of metastases at time of diagnosis were significant prognostic markers for overall and recurrence-free survival (Table 7; Fig. 6, *A-C*). Young age was significantly correlated with a good prognosis for overall survival but not for recurrence-free survival. On the other hand, histological subtype had no prognostic relevance in our cohort (Table 7). Together, this study confirms well-established clinicopathological parameters as prognostic markers.

Among the molecular markers, the p53 mutation status proved to be a strong prognostic marker for overall and recurrence-free survival in our ovarian carcinoma cohort ($P = 0.019$ and $P = 0.006$, respectively; Table 7; Fig. 6*D*). Although 17 of 23 patients (74%) with p53 wild-type tumors were still alive at the last follow-up, only 6 of 23 wild-type patients (26%) had died. In contrast, only 28 of 66 patients (42%) with p53 mutant tumors were still alive, whereas 38 of 66 (57%) mutant patients had died. The median overall survival time was 91 months in the p53 wild-type group, compared with only 61 months in the p53 mutant group. TAp73, Ex2p73, and Ex2/3p73 were not

Table 4 *Relationship between p53 mutation status and p73 up-regulation*

Tumor upregulation is defined as above the 75th percentile of the normal group.

Tumor	% of patients
Wild-type p53	
ΔNp73 upregulation	48% (11/23)
ΔN′p73 upregulation	96% (22/23)
TAp73 upregulation	96% (22/23)
Mutant p53	
ΔNp73 upregulation	23% (16/69)
ΔN′p73 upregulation	82% (56/68)
TAp73 upregulation	96% (65/68)

Table 5 *Relationship between p73 isoform expression and clinical parameters*

For correlation of ordinal or continuous clinical variables (tumor stage, tumor grade, residual disease after resection, age), the Spearman Rank test was used and the Spearman Rank Correlation Coefficient is given (*P* in brackets). For correlation of categorical variables (histological subtype, metastases), the Kruskal-Wallis test was used. Median and range are given (*P* in brackets).

Clinical parameters	No. of cases ($n = 96$)[a]	Measures for associations (*P*)				
		TAp73	ΔN′p73	ΔNp73	Ex2p73	Ex2/3p73
Age at diagnosis	95	−0.065	−0.055	0.137	0.118	0.089
		(0.532)	(0.597)	(0.184)	(0.253)	(0.393)
Tumor stage						
1	20	0.148	0.167	0.136	−0.034	−0.015
2	5	(0.153)	(0.110)	(0.190)	(0.745)	(0.885)
3	58					
4	11					
Tumor grade						
1	2	−0.110	−0.164	−0.091	0.059	−0.011
2	55	(0.303)	(0.125)	(0.394)	(0.579)	(0.918)
3	35					
Residual disease after surgical treatment						
None	35	0.025	0.004	−0.064	−0.121	−0.061
<2 cm	27	(0.812)	(0.973)	(0.548)	(0.254)	(0.569)
>2 cm	27					
Histological subtype[b]						
Serous	35	334, 31–3043	73, 0–794	21, 0–413	22, 2–280	407, 24–22826
Mucinous	39	368, 42–7921	63, 8–1325	18, 1–2947	20, 1–306	370, 46–12089
Endometroid	19	361, 33–4315	51, 9–551	9, 0–1388	22, 3–269	286, 32–17800
		(0.816)	(0.545)	(0.484)	(0.944)	(0.780)
Distant metastases						
Yes	11	347, 154–1999	81, 14–551	13, 0–294	9, 6–280	327, 94–1957
No	85	361, 381–7921	65, 0–1325	19, 0–2947	22, 1–392	405, 24–72798
		(0.687)	(0.463)	(0.306)	(0.546)	(0.476)

[a] Due to missing values in a few cases, numbers do not add up to a total of 96 patients in every category.
[b] Due to small numbers, the histological subtypes "clear cell adenocarcinoma" ($n = 2$) and "undifferentiated carcinoma" ($n = 1$) have been excluded from statistical analysis.

correlated with survival (Table 7). Because ΔNp73/ΔN′p73 transcripts produce the same polypeptide and are overexpressed in all tumors, values were pooled, and tumors were arbitrarily divided by median tumor levels into two approximately evenly sized subgroups (above and below the 50th percentile of the range of Np73/ΔN′p73 expression). A trend was seen for better overall survival in ovarian carcinoma patients with low expression of ΔN′p73/ΔNp73, compared with patients with high expression ($P = 0.1175$; Table 7; Fig. 6*E*). However, this trend did not reach statistical significance. Finally, in multivariate survival analysis, only residual disease after resection remained as a significant prognostic marker for overall survival.

DISCUSSION

Here we provide the largest and most comprehensive tumor expression analysis of all NH_2-terminal p73 isoforms reported to date, encompassing 100 ovarian carcinomas of all histological types, and evaluate their correlation to clinicopathological parameters. We used a highly reproducible quantitative RT-PCR assay optimized for product specificity and sensitivity. The most striking finding is the high prevalence of up-regulation of ΔN′p73 in the vast majority of ovarian carcinomas (95% of cases), providing a molecular marker of this disease. ΔN′p73 is derived from the P1 promoter. The importance of tumor-specific up-regulation of ΔN′p73 was hinted previously in a small semi-quantitative study of hepatocellular carcinomas that found ΔN′p73 up-regulation in six of six tumors (18). In contrast, up-regulation of the P2 promoter-derived ΔNp73 transcript was present in a small subgroup of 26% of ovarian carcinomas. We conclude that ΔN′p73, rather than ΔNp73, is the main contributor to total ΔNp73 up-regulation in ovarian cancers. Thus, the P1 promoter rather than the P2 promoter is primarily deregulated, at least in this cancer type. Our data also reveal differential *in vivo* regulation among the various P1 promoter-derived isoforms. Although ΔN′p73 is up-regulated in almost all ovarian cancers, and TAp73 is up-regulated in about one-third, Ex2/3p73 levels are actually down-regulated, possibly because of down-regulation of the splice acceptor on exon 4 at the pre-mRNA level (29). Expression data of Ex2/3p73 in human cancers had not been reported previously. Ex2p73 levels remained largely unchanged. Taken together, Ex2 and Ex2/3p73 isoforms do not seem to play a major oncogenic role in ovarian carcinogenesis. Six percent of tumors showed ΔNp73 expression levels that exceeded the highest normal ΔNp73 values, reflecting up-regulation of the P2 promoter at least in

Table 6 *Mutant p53 status is associated with tumor grade, histological type and metastasis*

For differences between wild-type and mutant p53 status regarding age, the Kruskal-Wallis test is used. For differences regarding the categorical variables tumor stage, tumor grade, residual disease after resection, histological subtype, distant metastases, the χ^2 test was used.

Clinical parameters	No. of cases	p53 status		*P*
		Wild-type ($n = 24$[a])	Mutant ($n = 69$[a])	
Age at diagnosis				
Median age (range)		66 (24–90)	61 (36–84)	
Average age ± SD		62 ± 16	61 ± 11	0.385
Tumor stage				
1	17	7 (32%)	10 (15%)	
2	5	1 (5%)	4 (6%)	
3	54	13 (59%)	41 (63%)	
4	11	1 (5%)	10 (15%)	0.271
Tumor grade				
1	2	1 (4%)	1 (2%)	
2	48	21 (91%)	27 (44%)	
3	35	1 (4%)	34 (55%)	<0.001
Residual disease after resection				
None	30	9 (41%)	21 (34%)	
<2 cm	26	10 (46%)	16 (26%)	
>2 cm	27	3 (14%)	24 (39%)	0.068
Histological subtype[b]				
Serous	33	6 (27%)	27 (42%)	
Mucinous	36	14 (64%)	22 (34%)	
Endometrioid	17	2 (9%)	15 (23%)	0.05
Distant metastases				
Yes	11	0	11 (17%)	
No	78	23 (100%)	55 (83%)	0.036

[a] Because of missing values in a few cases, numbers do not add up to a total of 24 for wild-type tumors or 69 for mutant tumors for every clinical parameter.
[b] Due to small numbers, the histological subtypes "clear cell adenocarcinoma" ($n = 2$) and "undifferentiated carcinoma" ($n = 1$) have been excluded from statistical analysis.

Table 7 *Overall and recurrence-free survival in relation to clinical parameters and p73 isoform expression, univariate analyses*

		Overall survival (OS)				Recurrence-free survival (RFS)			
		Survival status				Recurrence			
	No. of cases ($n = 96$)[a]	Alive ($n = 50$)	Dead ($n = 46$)	Mean OS time in month, 95% confidence interval	*P*	No ($n = 54$)	Yes ($n = 42$)	Mean RFS time in month, 95% confidence interval	*P*
Age at diagnosis					0.008				
<25 percentile (51 years)	23	16	7	90 (69–111)		17	6	84 (65–103)	
25–50 percentile (62 years)	24	15	9	85 (67–103)		12	12	56 (39–73)	
50–75 percentile (73 years)	24	9	15	54 (35–73)		11	13	43 (27–59)	
>75 percentile	24	10	14	48 (30–67)		14	10	57 (35–80)	
Tumor stage					0.024				<0.001
1 + 2	25	18	7	93 (74–113)		23	2	101 (88–113)	
3	58	27	31	64 (51–77)		26	32	52 (39–65)	
4	11	4	7	40 (19–62)		3	8	24 (11–37)	
Tumor grade					0.019				0.001
1 + 2	57	35	22	83 (69–97)		41	16	80 (67–93)	
3	35	15	20	53 (36–70)		13	22	34 (23–46)	
Residual disease after resection					<0.001				<0.001
None	35	25	10	94 (77–110)		30	5	93 (80–106)	
<2 cm	27	18	9	77 (58–95)		17	10	72 (52–91)	
>2 cm	28	5	23	36 (25–47)		5	23	22 (13–31)	
Histological subtype					0.325				0.127
Serous	35	18	17	66 (49–83)		15	20	49 (32–66)	
Mucinous	39	17	22	66 (51–82)		25	14	69 (52–85)	
Endometrioid	19	14	5	83 (63–103)		13	6	58 (43–73)	
Distant metastases					0.01				0.002
Yes	11	3	8	35 (15–54)		2	9	20 (8–32)	
No	85	47	38	75 (64–86)		52	33	67 (56–79)	
p53 status					0.019				0.006
Wild type	23	17	6	91 (71–111)		19	4	64 (52–76)	
Mutant	66	28	38	61 (48–73)		29	37	46 (35–57)	
TAp73[b]					0.435				0.632
<50 percentile	47	26	21	76 (61–91)		28	19	64 (49–80)	
>50 percentile	49	24	25	62 (49–76)		26	23	57 (43–70)	
ΔNp73					0.826				0.556
<50 percentile	46	23	23	63 (50–76)		27	19	64 (49–79)	
>50 percentile	50	27	23	74 (59–90)		27	23	60 (45–75)	
ΔN′p73					0.281				0.909
<50 percentile	46	26	20	76 (60–91)		26	20	61 (46–77)	
>50 percentile	49	23	26	63 (49–76)		27	22	58 (45–72)	
Ex2p73					0.886				0.93
<50 percentile	47	22	25	68 (54–83)		26	21	62 (47–77)	
>50 percentile	49	28	21	72 (56–88)		28	21	47 (36–58)	
Ex2/3p73					0.467				0.709
<50 percentile	49	23	26	63 (50–75)		28	21	64 (50–79)	
>50 percentile	47	27	20	76 (60–92)		26	21	45 (35–55)	
ΔNp73/ΔN′p73[c]					0.12				0.552
<50 percentile	46	27	19	79 (63–94)		27	19	62 (46–77)	
>50 percentile	49	22	27	60 (46–74)		26	23	61 (46–76)	

[a] Due to missing values in a few cases, numbers do not add up to a total of 96 patients in every category.
[b] For each p73 isoform, two patient groups of approximately the same size were formed, one expressing above the 50th percentile and one expressing below the 50th percentile of the mean tumor levels.
[c] The variable ΔNp73/ΔN′p73 was obtained by adding the copy numbers.

some tumors. This increase in tumor ΔNp73 levels might be a reflection of the previously suggested autoregulatory feedback loop of p53 and TAp73 inducing the P2 promoter (17, 22, 30, 31). Consistent with this notion, 17 of 21 ovarian cancers with the highest ΔNp73 levels also exhibited high TAp73 levels; in addition, 8 of these 17 tumors were wild type for p53.

Another novel result of this study is the strong correlation between p53 status and up-regulation of dominant-negative ΔN/ΔN′p73 in tumors. The fact that ovarian cancers select ΔN′p73 and ΔNp73 in 95% and 26% of tumors, respectively, is by itself a strong argument for their oncogenic role *in vivo*. Up-regulation of these isoforms could bestow oncogenic activity on the TP73 gene, because they interfere with the tumor suppressor functions of p53 and TAp73. To test whether the TP73 gene might function to counteract the mutational selection pressure for TP53, we reasoned that if ΔTAp73 isoforms were indeed oncogenic inhibitors of p53 and TAp73 *in vivo*, their up-regulation should occur preferentially in wild-type p53 tumors. Our results indeed support this notion. We found significantly higher expression levels of ΔNp73, ΔN′p73, and Ex2/3p73 (as well as TAp73) in p53 wild-type ovarian cancers than in p53 mutant cancers (Fig. 5). Moreover, the prevalence of up-regulation for ΔNp73 and ΔN′p73 was higher in wild-type tumors than in mutant tumors (48% and 96% *versus* 23% and 82%; Table 4). On the other hand, no difference was seen in the prevalence of TAp73 up-regulation between wild-type and mutant tumors (Table 4). This result further solidifies our previous result on a series of gynecological tumors, where we already saw a strong statistical trend between tumor-specific up-regulation of ΔTAp73 isoforms and wild-type p53 status (19). Together, these *in vivo* data provide compelling evidence for the notion that expression of dominant-negative ΔTAp73 can alleviate the selection pressure for p53 during tumor formation.

What, if any, is the impact of concomitantly increased TAp73 expression in tumorigenesis? Apparently, cancer cells can tolerate increased levels of this proapoptotic protein, because high TAp73 expression in tumors is neutralized by increased levels of transdominant ΔTAp73. We and others recently showed that physical interaction between oncogenic and antioncogenic family members is one of the possible mechanisms of interference with the specific DNA binding activity of wild-type p53 and TAp73. Inactive mixed protein complexes were found between endogenous ΔNp73α or ΔNp73β on

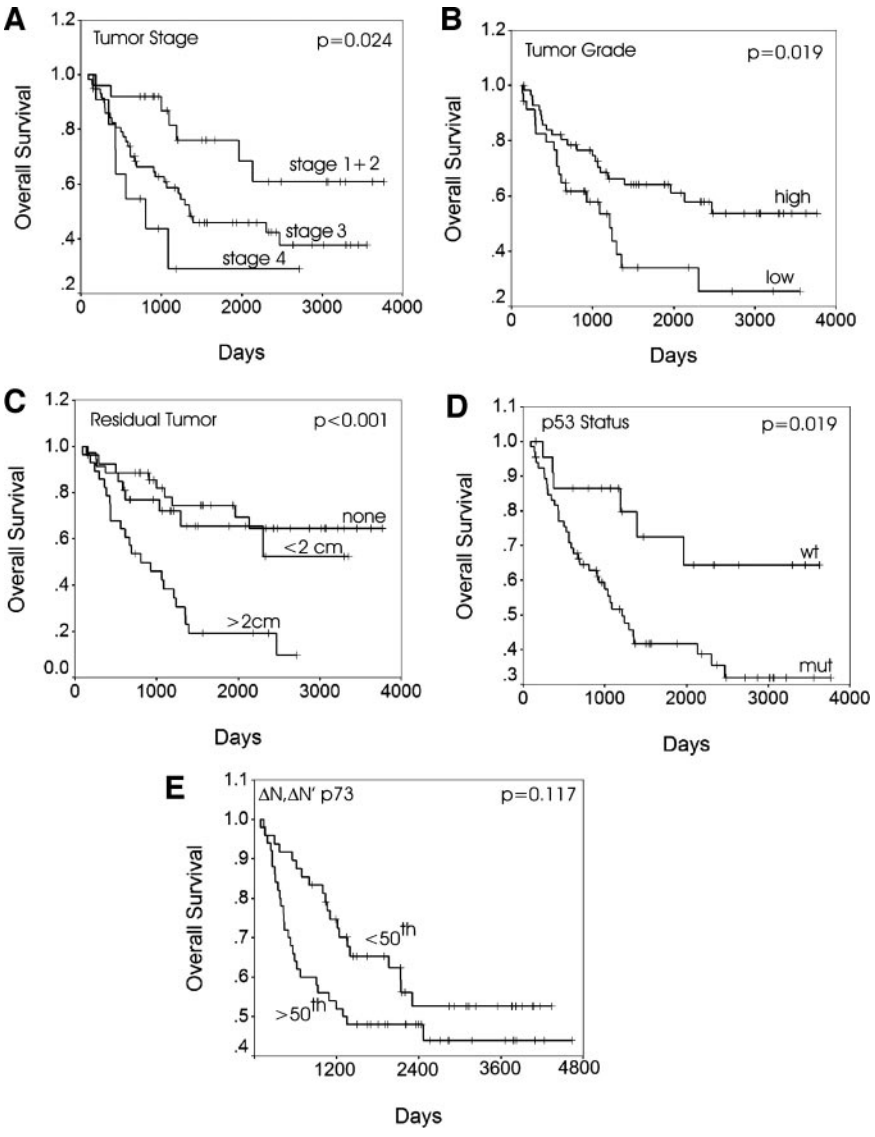

Fig. 6. Kaplan-Meier survival curves in 96 ovarian carcinomas of all histotypes for tumor stage (*A*), tumor grade (*B*), residual tumor after resection (*C*), p53 mutation status (*D*), and ΔN′p73/ΔNp73 levels (*E*) at time of diagnosis.

the one hand and wild-type p53 or TAp73α or β on the other hand in primary human tumors, cultured tumor cells, and mouse neuronal cultures (14, 17, 19, 32). Of note, a stoichiometry as low as 1:3 of mutant to wild-type p53 molecules in heterozygous tumors abrogates wild-type function, suggesting that a similarly skewed stoichiometry might be effective for mixed ΔNp73 complexes as well. An additional mechanism of inhibition might be direct promoter competition, with ΔNp73 displacing wild-type p53 or TAp73 from their DNA binding sites (21). Thus, a slight decrease in the TA/ΔTA ratio might be sufficient to convert TP73 from a tumor suppressor into an oncogene. Interestingly, a strong prognostic impact of ΔNp73 up-regulation could be shown in neuroblastoma, notably one of the rare tumor types that show no selection pressure at all for p53 (25). In addition to aberrant subcellular localization of wild-type p53 as an important mechanism to circumvent mutational pressure (33, 34), ΔNp73-mediated inhibition could be a second contributing factor to the virtual absence of p53 mutations in neuroblastoma. A third mechanism that allows cancer cells to tolerate high TAp73 levels could be mediated through p53 mutants, because certain tumor-derived p53 mutant proteins associate with and inhibit TAp73 function in cultured cells (6, 35).

Taken together, a unifying interpretation of our findings is that the P1 promoter of TP73 is up-regulated in ovarian cancer, possibly via deregulated E2F activity or other mitogenic oncogenes. E2F1 is a direct transcriptional activator of the P1 promoter of TP73 (7–10), and deregulated E2F1 activity is an almost universal hallmark of human cancers (36). Furthermore, the biologically relevant target of P1 up-regulation might be the oncogenic ΔN′p73, whereas the opposing TAp73 might be a "side product" that becomes co-up-regulated by default but is functionally neutralized by ΔN′p73. A second route for self-inactivation of TAp73 exists through ΔNp73, produced via the autoregulatory loop. Our finding that ΔTAp73 up-regulation is significantly correlated with wild-type p53 tumor status strengthens the hypothesis that these isoforms provide a pathway for epigenetic inactivation of wild-type p53 in tumors and thus act as oncogenes *in vivo*.

Evidence from tissue culture and mouse studies is mounting that ΔNp73 protein might function as an oncogene in human cancer (15, 18, 19, 23). Ideally, the strongest endorsement for a tumor-promoting role of any candidate human oncogene is a direct impact on survival. Thus, studies addressing the clinical relevance of ΔNp73 in human cancer will be of high importance. To date, only one study, performed in 52 neuroblastoma patients, has found that the presence of ΔN/ΔN′p73 expression is a significant prognostic marker for overall and

recurrence-free survival ($P < 0.001$), independent of age, tumor stage, primary tumor site, and N-Myc amplification (25). In the neuroblastoma study, combined ΔN/ΔN′p73 was detectable in 30% of tumors. Tumors expressing both TA and ΔN/ΔN′p73 isoforms had variable ratios, with TAp73 being the prevalent variant. Although TAp73 had no effect on survival, the expression of the ΔN/ΔN′p73 had a strong negative impact on survival of these neuroblastoma patients. In contrast, in our cohort of ovarian cancers, up-regulation of ΔN′p73, defined as levels ranging above the 75th percentile of normal levels, was a molecular marker of the tumorous condition per SE, because it occurred in every cancer. Thus, in contrast to neuroblastoma, the presence or absence of ΔN/ΔN′p73 up-regulation does not stratify ovarian cancer patients, because it occurs universally. To determine whether the degree of up-regulation of ΔNp73/ΔN′p73 contained further prognostic information for survival, tumors were arbitrarily divided by median tumor levels into two subgroups. In support of the findings in neuroblastoma patients, a trend was seen for better overall survival in ovarian carcinoma patients with low expression of ΔN′p73/ΔNp73, compared with patients with high expression (Table 7; Fig. 6*E*). Moreover, as in neuroblastoma, TAp73 expression levels showed no correlation with survival. Although our study falls short of demonstrating prognostic significance for ΔN′p73/ΔNp73, it is important to keep in mind that in sharp contrast to neuroblastoma, 74% of our ovarian carcinoma patients harbored p53 mutations, and these mutations already contributed to poor clinical outcome (Fig. 6*D*). Thus, the "need" for epigenetic inhibition of p53/TAp73 by deregulated ΔN′p73/ΔNp73 in this cohort was diminished. It is therefore tempting to speculate that ΔN′p73/ΔNp73 might be of prognostic value in the subgroup of ovarian carcinomas that retains wild-type p53, such as *e.g.*, the endometrioid type. Our results are also consistent with the two previous p73 ovarian cancer studies reported. Both determined global p73 expression that did not distinguish between TA and ΔTA isoforms, using immunohistochemistry or semi-quantitative RT-PCR. Nevertheless, high p73 expression correlated with advanced tumor stage (37, 38) and poorer survival (37). Using the isoform-specific assay developed here to design larger studies in the future will allow for a definitive answer on whether N′p73/ΔNp73 is an independent prognostic marker for ovarian cancer.

ACKNOWLEDGMENTS

We thank A. Kuehler, B. Rosati, F. Grau, P. Pancoska and E. Schuster for technical assistance.

REFERENCES

1. Jost CA, Marin MC, and Kaelin WG Jr. p73 is a simian [correction of human] p53-related protein that can induce apoptosis. Nature (Lond) 1997;389:191–4.
2. Vousden KH, Lu X. Live or let die: the cell's response to p53. Nat Rev Cancer 2002;2:594–604.
3. Zhu J, Jiang J, Zhou W, Chen X. The potential tumor suppressor p73 differentially regulates cellular p53 target genes. Cancer Res 1998;58:5061–5.
4. Agami R, Blandino G, Oren M, Shaul Y. Interaction of c-Abl and p73α and their collaboration to induce apoptosis. Nature (Lond) 1999;399:809–13.
5. Gong JG, Costanzo A, Yang HQ, et al. The tyrosine kinase c-Abl regulates p73 in apoptotic response to cisplatin-induced DNA damage. Nature (Lond) 1999;399: 806–9.
6. Bergamaschi D, Gasco M, Hiller L, et al. p53 polymorphism influences response in cancer chemotherapy via modulation of p73-dependent apoptosis. Cancer Cell 2003; 3:387–402.
7. Irwin M, Marin MC, Phillips AC, et al. Role for the p53 homologue p73 in E2F-1-induced apoptosis. Nature (Lond) 2000;407:645–8.
8. Lissy NA, Davis PK, Irwin M, et al. A common E2F-1 and p73 pathway mediates cell death induced by TCR activation. Nature (Lond) 2000;407:642–5.
9. Stiewe T, Putzer BM. Role of the p53-homologue p73 in E2F1-induced apoptosis. Nat Genet 2000;26:464–9.
10. Zaika A, Irwin M, Sansome C, Moll UM. Oncogenes induce and activate endogenous p73 protein. J Biol Chem 2001;276:11310–6.
11. Melino G, De Laurenzi V, Vousden KH. p73: friend or foe in tumorigenesis. Nat Rev Cancer 2002;2:605–15.
12. Yang A, Walker N, Bronson R, et al. p73-deficient mice have neurological, pheromonal and inflammatory defects but lack spontaneous tumours. Nature (Lond) 2000; 404:99–103.
13. Moll UM, Erster S, Zaika A. p53, p63 and p73–solos, alliances and feuds among family members. Biochim Biophys Acta 2001;1552:47–59.
14. Pozniak CD, Radinovic S, Yang A, McKeon F, Kaplan DR, Miller, FD. An anti-apoptotic role for the p53 family member, p73, during developmental neuron death. Science (Wash D C) 2000;289:304–6.
15. Ishimoto O, Kawahara C, Enjo K, Obinata M, Nukiwa T, Ikawa S. Possible oncogenic potential of DeltaNp73: a newly identified isoform of human p73. Cancer Res 2002;62:636–41.
16. Kaghad M, Bonnet H, Yang A, Creancier L, Biscan JC, Valent A, et al. Monoallelically expressed gene related to p53 at 1p36, a region frequently deleted in neuroblastoma and other human cancers. Cell 1997;90:809–19.
17. Nakagawa T, Takahashi M, Ozaki T, et al. Autoinhibitory regulation of p73 by Delta Np73 to modulate cell survival and death through a p73-specific target element within the Delta Np73 promoter. Mol Cell Biol 2002;22:2575–85.
18. Stiewe T, Zimmermann S, Frilling A, Esche H, Putzer BM. Transactivation-deficient DeltaTA-p73 acts as an oncogene. Cancer Res 2002;62:3598–602.
19. Zaika AI, Slade N, Erster SH, et al. ΔNp73, a dominant-negative inhibitor of wild-type p53 and TAp73, is up-regulated in human tumors. J Exp Med 2002;196: 765–80.
20. Fillippovich I, Sorokina N, Gatei M, et al. Transactivation-deficient p73alpha (p73Deltaexon2) inhibits apoptosis and competes with p53. Oncogene 2001;20: 514–22.
21. Stiewe T, Theseling CC, Putzer BM. Transactivation-deficient Delta TA-p73 inhibits p53 by direct competition for DNA binding: implications for tumorigenesis. J Biol Chem 2002;277:14177–85.
22. Grob TJ, Novak U, Maisse C, et al. Human delta Np73 regulates a dominant negative feedback loop for TAp73 and p53. Cell Death Differ 2001;8:1213–23.
23. Petrenko O, Zaika A, Moll UM. ΔNp73 facilitates cell immortalization and cooperates with oncogenic Ras in cellular transformation in vivo. Mol Cell Biol 2003;23: 5540–55.
24. Stiewe T, Stanelle J, Theseling CC, Pollmeier B, Beitzinger M, Putzer BM. Inactivation of the RB tumor supressor gene by oncogenic isoforms of the p53 family member p73. J Biol Chem 2003;278:14230–6.
25. Casciano I, Mazzocco K, Boni L, et al. Expression of ΔNp73 is a molecular marker for adverse outcome in neuroblastoma patients. Cell Death Differ 2002;9:246–51.
26. de Leeuw WJ, Slagboom PE, Vijg J. Quantitative comparison of mRNA levels in mammalian tissues: 28S ribosomal RNA level as an accurate internal control. Nucleic Acids Res 1989;17:10137–8.
27. Flaman JM, Frebourg T, Moreau V, et al. A simple p53 functional assay for screening cell lines, blood, and tumors. Proc Natl Acad Sci USA 1995;92:3963–7.
28. Kovalev S, Marchenko N, Swendeman S, LaQuaglia M, Moll UM. Expression level, allelic origin, and mutation analysis of the p73 gene in neuroblastoma tumors and cell lines. Cell Growth Differ 1998;9:897–903.
29. Mercatante, DR, and Kole R. Control of alternative splicing by antisense oligonucleotides as a potential chemotherapy: effects on gene expression. Biochim Biophys Acta 2002;1587:126–32.
30. Kartasheva NN, Contente A, Lenz-Stoppler C, Roth J, Dobbelstein M. p53 induces the expression of its antagonist p73 ΔN, establishing an autoregulatory feedback loop. Oncogene 2002;21:4715–27.
31. Vossio S, Palescandolo E, Pediconi N, et al. DN-p73 is activated after DNA damage in a p53-dependent manner to regulate p53-induced cell cycle arrest. Oncogene 2002;21:3796–803.
32. Slade N, Zaika AI, Erster S, Moll UM. ΔNp73 stabilises TAp73 proteins but compromises their function due to inhibitory hetero-oligomer formation. Cell Death Differ [serial on the Internet]. 2003 Dec 12 [Epub ahead of print]. 2003;doi:10.1038/sj.cdd. 4401335.
33. Moll UM, LaQuaglia M, Benard J, Riou G. Wild-type p53 protein undergoes cytoplasmic sequestration in undifferentiated neuroblastomas but not in differentiated tumors. Proc Natl Acad Sci USA 1995;92:4407–11.
34. Nikolaev AY, Li M, Puskas N, Qin J, Gu W. Parc: a cytoplasmic anchor for p53. Cell 2003;112:29–40.
35. Gaiddon C, Lokshin M, Ahn J, Zhang T, Prives C. A subset of tumor-derived mutant forms of p53 down-regulate p63 and p73 through a direct interaction with the p53 core domain. Mol Cell Biol 2001;21:1874–87.
36. Cotran RS, Collins T, Robbins SL. Pathologic basis of diseases, 6th edition. Philadelphia, PA: W.B. Saunders Co.; 1999. p. 279.
37. Niyazi M, Ghazizadeh M, Konishi H, Kawanami O, Sugisaki Y, Araki T. Expression of p73 and c-Abl proteins in human ovarian carcinomas. J Nippon Med Sch 2003; 70:234–42.
38. Chen CL, Ip SM, Cheng D, Wong LC, Ngan, HY. P73 gene expression in ovarian cancer tissues and cell lines. Clin Cancer Res 2000;6:3910–5.